Available online at www.sciencedirect.com
ScienceDirect
Polymer 48 (2007) 2613–2618
polymer
www.elsevier.com/locate/polymer

Polylactide compositions. Part 1: Effect of filler content and size on mechanical properties of PLA/calcium sulfate composites

Marius Murariu, Amália Da Silva Ferreira, Philippe Degée, Michael Alexandre, Philippe Dubois*

Laboratory of Polymeric and Composite Materials (LPCM), University of Mons-Hainaut, Place du Parc 20, 7000 Mons, Belgium

Received 28 November 2006; received in revised form 23 February 2007; accepted 28 February 2007
Available online 3 March 2007

Abstract

Starting from calcium sulfate (gypsum) as a fermentation by-product of lactic acid fermentation, novel high performance composites have been produced by melt-blending polylactide (PLA) and previously dried calcium sulfate hemihydrate in a Brabender bench scale kneader at 190 °C. Due to PLA sensitivity towards hydrolysis, it has first been demonstrated that formation of β-anhydrite II (AII) by adequate thermal treatment of calcium sulfate is a prerequisite. Then, the effect of filler content and mean diameter on thermal, mechanical and impact properties has been examined together with the morphology of the resulting materials. It shows that high tensile performances and impact strength are maintained up to a filler content of 20 wt% without any increase of PLA crystallinity. Interestingly enough and provided that AII particles with a mean diameter of ca. 10 μm were considered as PLA fillers, tensile and impact properties proved to be maintained at a very acceptable level at filler content as high as 50 wt%. Such remarkable mechanical behavior can be accounted for by the excellent filler dispersion throughout the polyester matrix and much favorable interactions between $CaSO_4$ particles and ester functions of PLA chains as evidenced by the use of predictive mathematical models for composite mechanical properties and SEM–BSE imaging of fractured surfaces.

Keywords: Poly(lactic acid); Calcium sulfate anhydrite; Composites

1. Introduction

Polylactide (PLA) has been widely studied for use in biomedical applications due to its bioresorbable and biocompatible properties in human bodies [1–3]. More recently, PLA has proved to be a cost-effective alternative to commodity petrochemical-based materials with advantages such as: (1) it can be obtained from renewable agricultural resources; (2) its production consumes CO_2 and provides significant energy savings; (3) it is recyclable and compostable; (4) physical and mechanical properties can be modified to a large extent through (stereo)control of PLA chains and related polymer architectures and combination with any relevant additives and/or fillers [4–8]. The basic constitutional unit of PLA, lactic acid (2-hydroxypropanoic acid), can be produced through chemical synthesis as a racemic mixture while lactic acid enantiomers are obtained by carbohydrate fermentation using appropriate bacterial strain. The fermentation broth containing lactate is filtered to remove cells, carbon treated, evaporated and acidified with sulfuric acid to get lactic acid. Further purification steps involve esterification, distillation and hydrolysis as depicted in Scheme 1. Such a procedure results in the formation of large amounts of calcium sulfate, i.e. gypsum, as main by-product [9]. Therefore, there is a need for new prospects in which gypsum can be made profitable and contribute to decrease lactic acid derivatives and PLA costs.

This paper aims at reporting on the preparation and characterization of PLA-based composites filled with calcium sulfate directly obtained from the lactic acid fermentation process. Due to the well-established PLA sensitivity towards hydrolysis, special care is to be taken by an adapted drying of native calcium sulfate (gypsum). The effect of dried calcium sulfate content and

* Corresponding author. Tel.: +32 65 37 34 80; fax: +32 65 37 34 84.
E-mail address: philippe.dubois@umh.ac.be (P. Dubois).

0032-3861/$ - see front matter © 2007 Elsevier Ltd. All rights reserved.
doi:10.1016/j.polymer.2007.02.067

(a) *Fermentation and neutralization*

$$C_6H_{12}O_6 + Ca(OH)_2 \rightarrow (CH_3\text{-}CH(OH)COO^-)_2Ca^{2+} + 2\,H_2O$$

(b) *Hydrolysis by H_2SO_4*

$$(CH_3\text{-}CH(OH)COO^-)_2Ca^{2+} + H_2SO_4 \rightarrow 2\,CH_3\text{-}CH(OH)COOH + CaSO_4\downarrow$$

(c) *Esterification*

$$CH_3\text{-}CH(OH)COOH + R\text{-}OH \rightarrow CH_3\text{-}CH(OH)COOR + H_2O$$

(d) *Hydrolysis by H_2O*

$$CH_3\text{-}CH(OH)COOR + H_2O \rightarrow CH_3\text{-}CH(OH)COOH + R\text{-}OH$$

Scheme 1. Sketch of lactic acid production by fermentation.

average size on thermal, mechanical and impact properties has been examined together with the morphology of the resulting composite materials. Although mineral fillers such as hydroxyapatite [10–12], calcium carbonate [13,14], calcium phosphate and other bioceramics [15–19] have already been used in combination with PLA for prosthetic purposes in bone tissue regeneration, to the best of our knowledge no comprehensive study has been published so far on PLA/calcium sulfate composites with mineral loading that can be as high as 50 wt%.

2. Experimental part

2.1. Materials

Polylactide (PLA, number average molar mass = 74,500, residual monomer content = 0.18%, D-isomer content = 4.3%, melt flow index (190 °C, 2.16 kg) = 6.61 g/10 min and density = 1.25 g/cm^3) was supplied by Galactic s.a. under the trade name: Galactic, and dried for 4 h at 110 °C under vacuum just before use. Calcium sulfate hemihydrate ($CaSO_4\cdot 0.5H_2O$) – a by-product obtained from the lactic acid fermentation process with mean particle diameters ranging from 9 to 43 μm was provided by Galactic s.a. and dried at various temperatures before melt-blending. Calcium sulfate anhydrite II (CAS-20-4) with an average diameter of 4 μm was kindly supplied by United States Gypsum Company.

2.2. Sample preparation

Starting from calcium sulfate hemihydrate, β-anhydrites II (AII) and III (AIII) were obtained by drying in a Nabertherm 3L furnace at 500 and 200 °C for 1 h, respectively. Composites were obtained by melt-compounding PLA pellets with up to 50 wt% of AII at 190 °C using a Brabender bench scale kneader equipped with cam blades for 3 min at 30 rpm, followed by 3 min at 60 rpm. Three-millimeter thick plates were then prepared by compression molding at 190 °C using an Agila PE20 hydraulic press (low pressure for 240 s with three degassing cycles, followed by a high-pressure cycle at 150 bars for 150 s and cooling by tap water at 50 bars). Specimens for tensile and Izod impact testing were cut from plates by using a milling-machine in accordance to ASTM D 638-02a norm (specimen type V) and ASTM D 256-A norm (specimens 60 × 10 × 3 mm), respectively.

2.3. Characterization

PLA molecular weight parameters (number average molar mass, M_n; polydispersity index, M_w/M_n) were determined by size exclusion chromatography (SEC) at 35 °C using a Polymer Laboratories (PL) liquid chromatograph equipped with a PL-DG802 degasser, a HPLC pump LC1120 (flow rate: 1 ml/min), a Basic-Marathon autosampler (injection volume = 200 μl from an initial 10 mg polymer solution in 5 ml THF previously filtered over 0.2 μm Acrodisc filter), a PL-RI refractive index detector and four columns: a guard column PL gel 10 μm (50 × 7.5 mm^2) and three columns PL gel 10 μm mixed-B (300 × 7.5 mm^2). M_n and M_w/M_n were calculated with reference to PS standards and using the Kuhn–Mark–Houwink relationship for PLA in THF [20]. The extraction of PLA chains from composite materials was carried out by selective PLA dissolution in $CHCl_3$, removal of insoluble calcium sulfate by filtration, liquid–liquid extraction of the organic supernatant with successively 0.1 M HCl aqueous solution and deionized water, and finally precipitation of PLA in a large volume of excess heptane. Differential scanning calorimetry (DSC) measurements were performed by using a DSC Q100 from TA Instruments under nitrogen flow (first heating ramp of 10 °C/min from 0 to 220 °C to eliminate a different thermal history after processing by compression molding, cooling ramp of 10 °C/min down to −10 °C to give samples a similar known thermal history, second heating ramp of 10 °C/min from −10 to 220 °C to record the events of interest and to compare polymer crystallization properties).

Glass transition temperature (T_g), melting temperature (T_m) and melting enthalpy (ΔH_m) were determined from the second heating cycle. The degree of crystallinity, expressed in J/g of PLA, was calculated by considering a melting enthalpy of 93 J/g for 100% crystalline PLA [21]. Thermogravimetry analyses (TGA) of PLA composites were performed by using a TGA Q50 from TA Instruments with a heating ramp of 20 °C/min under atmospheric air flow (platinum pans, 60 cm^3/min air flow rate).

"Drying–water absorption–drying" cycles from calcium sulfate hemihydrate as simulated by TGA were performed by using HiRes TGA 2950 from TA Instruments (platinum pans, air flow rate of 74 cm^3/min, approx. 50% R.H.). The first step with a heating ramp of 20 °C/min up to 200 (or 500 °C) was followed by 1 h isotherm at 200 (or 500 °C) to obtain anhydrite form AIII (or AII), cooling under air flow to get information about anhydrite stability directly followed by a second isotherm.

Tensile and impact tests were performed with a Lloyd LR 10K tensile bench in accordance to ASTM D 638-02a norm (crosshead speed = 1 mm/min), while Ray-Ran 2500 pendulum impact tester and a Ray-Ran 1900 notching apparatus were used in Izod mode according to ASTM D 256 norm (Method A). For both tensile and impact tests, specimens were previously conditioned for at least 48 h at 20 ± 1 °C under relative humidity of 45 ± 5% and values were averaged over five measurements.

Scanning electron microscopy (SEM) was performed on samples' surface previously fractured at liquid nitrogen

temperature by using a scanning electronic microscope Philips XL at an accelerated voltage of up to 30 kV and various magnitudes. SEM was equipped for both secondary electron (SE) and back scattered electron (BSE) imaging.

3. Results and discussion

Like other polyesters, polylactide (PLA) is stable in the molten state provided that it is adequately stabilized and intensively dried before processing with a maximum acceptable water content of 250 ppm [22]. Therefore, it is of prime importance to dry the polyester resin and also calcium sulfate hemihydrate ($CaSO_4 \cdot 0.5H_2O$) prior to melt-compounding. As exemplified in the literature, drying gypsum under atmospheric pressure above 100 °C favors β-calcium sulfate hemihydrate formation. Further increasing the temperature allows producing instable β-anhydrite III (AIII) (formed at 200 °C) and stable β-anhydrite II (AII) generated at 500 °C [23–27]. TGA isotherms performed at 200 and 500 °C attest for the rapid weight loss of water (ca. 7.5 wt% within 10 min) of calcium sulfate hemihydrate yielding anhydrite forms AIII and AII, respectively (Fig. 1A and B). Furthermore and after 1 h isotherm at 200 and 500 °C, both anhydrite forms have undergone a cooling step under air flow directly followed by a second isotherm. Clearly AIII, i.e., the instable β-anhydrite form obtained upon heating at 200 °C, reabsorbs rapidly ambient moisture forming back calcium sulfate hemihydrate. Interestingly, anhydrite II (AII, thus formed at 500 °C) remains quite stable. In order to confirm this observation, 20 g of previously dried AIII and AII have been left under atmospheric conditions for 24 h and the relative rate of water reabsorption has been determined by weighing. After 2 h exposure time, water uptake reaches 0.8 wt% for AII (only 1.1 wt% even after 24 h) compared to 7.5 wt% for AIII (Fig. 2). It can thus be concluded that the β-anhydrite form AII is much better suited for being melt-blending with PLA than AIII, which is by far too sensitive to atmospheric water absorption.

In a second step, PLA/AII compositions with filler contents up to 50 wt% have been prepared by melt-blending at 190 °C using a Brabender bench scale kneader and compression molding as 3-mm thick plates. Table 1 shows the effect of processing conditions and filler loading on PLA molecular parameters (number average molar mass, M_n; polydispersity, M_w/M_n). For sake of comparison, compositions produced with 20 wt% of AIII and calcium sulfate hemihydrate are also presented (entries 8 and 9). It comes out that addition of AII to PLA does not lead to important modifications of molar mass and molar masses distribution, at least within experimental errors which can be estimated to 15% taking into account size exclusion chromatography accuracy but also PLA extraction and purification steps (see Section 2). Processing PLA at 190 °C exhibits a higher effect on M_n than addition of AII due to the inherent thermal sensitivity of PLA and the occurrence of transesterification reactions at such high compounding temperature. In contrast, the melt-blending PLA with mineral fillers (AIII

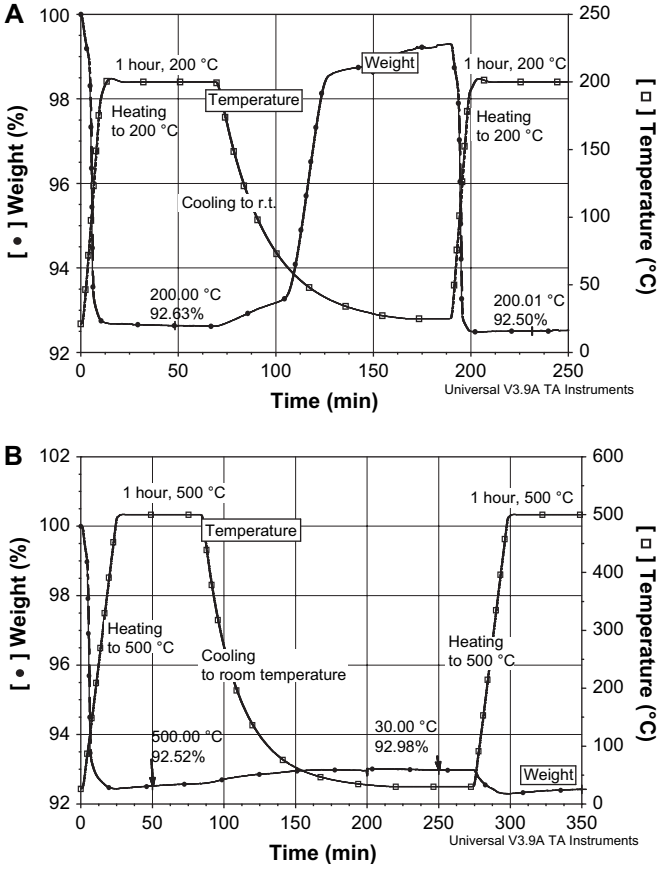

Fig. 1. "Drying–water absorption–drying" cycle as determined by TGA from calcium sulfate hemihydrate: (A) isotherms at 200 °C forming AIII and (B) isotherms at 500 °C leading to AII.

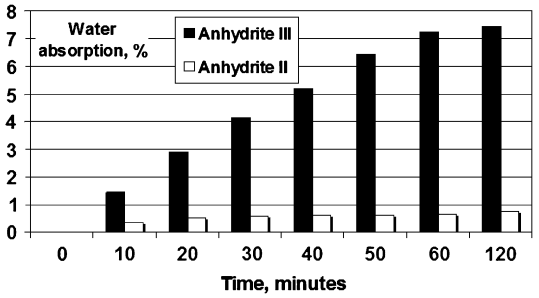

Fig. 2. Time dependence of water uptakes recorded for AII and AIII under atmospheric conditions.

Table 1
Dependence of PLA molecular parameters upon composite formation

Entry	Composition (wt/wt)	M_{nPLA}	M_w/M_n
1	Pristine PLA pellets	74,500	2.1
2	Processed PLA	64,000	2.2
3	PLA/AII (90/10)	70,000	2.2
4	PLA/AII (80/20)	59,000	2.4
5	PLA/AII (70/30)	62,000	2.4
6	PLA/AII (60/40)	63,000	2.2
7	PLA/AII (50/50)	62,000	2.3
8	**PLA/AIII (80/20)**	**46,000**	**2.4**
9	**PLA/$CaSO_4 \cdot 0.5H_2O$ (80/20)**	**38,500**	**3.1**

and calcium sulfate hemihydrate) containing adsorbed water triggers substantial decrease in M_n and increase in M_w/M_n, attesting for undesirable hydrolysis reaction of the aliphatic polyester chains.

Fig. 3 shows typical DSC thermograms of neat PLA and PLA/AII (60/40 by weight) as obtained after processing by compression molding (storage period of at least 48 h under anhydrous conditions). The results recorded during first DSC heating cycle attest that the performed compositions are characterized by similar cold crystallization properties. It could be concluded that addition of AII with a mean diameter of 9 μm does not promote any significant change in PLA crystallinity, which is likely related to the poor crystallization ability of the investigated PLA, i.e., actually containing 4.3 mol% of D-lactide unit. On the other hand, by controlled cooling (10 °C/min rate) from 220 °C to −10 °C, the crystallization of the materials could not be observed during DSC cooling cycle.

In Table 2, the effect of filler content on thermal transitions, melting enthalpy and degree of crystallinity during the second heating cycle is shown. It comes out that the cold crystallization is not observed by opposition to the first heating scan while increasing AII content only slightly enhances the degree of crystallinity from 0.1% to 2.3%. As far as TGA measurements are concerned, no increase in thermal instability of PLA is induced by the presence of β-anhydrite II. On the contrary, a slight increase of the maximum decomposition temperature is even observed from 375 to 400 °C by dispersing 50 wt% AII in PLA. Actually and it will be reported in a forthcoming paper, the morphology of a given microfiller has a significant importance. Fillers characterized by platelet-like primary particles, e.g. AII particles, are much favorable for the improvement of thermal stability compared to fillers (of same chemical composition) characterized by more isotropic geometry like spherical primary particles.

Note that a good agreement between the initial feed and experimental filler content in the recovered compositions has been obtained from the weight loss at 600 °C.

Tensile properties of unfilled PLA and PLA/AII composites have been measured by stress–strain experiments at room temperature (r.t.) after previous conditioning for at least 48 h (see Section 2). Fig. 4 shows the effect of the mean diameter of the dried calcium sulfate hemihydrate on both stress at break and Young's modulus for a constant PLA/AII (70/30) composition. It shows that higher performances are obtained for particle size close to 10 μm. Therefore, further characterizations by tensile and impact testings have been carried out with previously dried calcium sulfate hemihydrate of 9 μm mean diameter. From Table 3, it can be seen that both stress and nominal strain at break gradually decrease with filler content passing from 61 to 35 MPa and 9.2% to 2.5%, respectively. In contrast, Young's modulus increases with loading degree reaching ca. 750 MPa for 50 wt% AII.

In order to evaluate the affinity between the PLA matrix and AII particles, the recorded tensile data points have been compared with prediction values using two classical models: Einstein's Eq. (1) and Nicolais–Narkis general form (2) [28,29]:

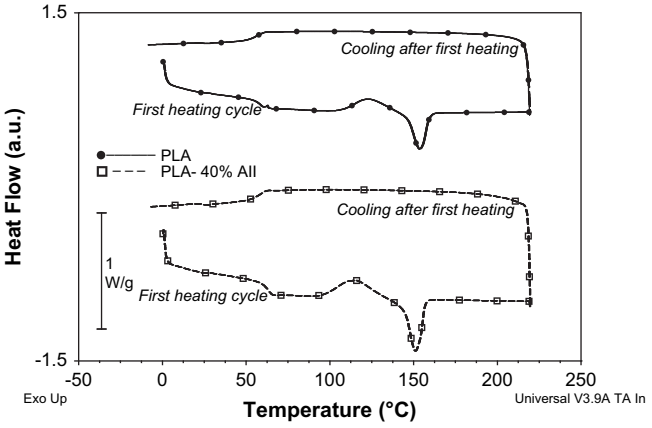

Fig. 3. DSC curves of unfilled PLA compared to PLA/AII (60/40 wt/wt) composite during the first heating cycle (see Section 2).

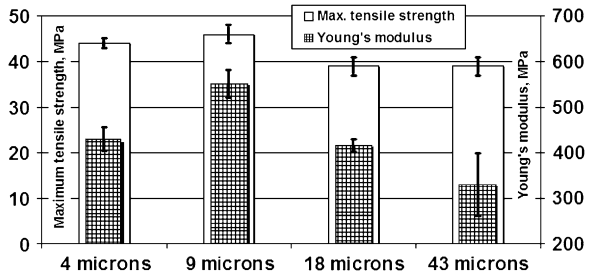

Fig. 4. Effect of filler mean diameter on tensile strength and modulus of PLA/AII (70/30) compositions as obtained by stress–strain experiments at r.t. (crosshead speed = 1 mm/min).

Table 2
DSC data of PLA (pristine granules and processed sample) and PLA/AII compositions (second heating scan from −10 to 220 °C with a ramp of 10 °C/min)

Compositions	T_g (°C)	T_m (°C)	ΔH_m (J g^{-1})	Crystallinity degree (%)
PLA granules	62.5	–	–	–
Processed PLA	62.0	153.0	0.13	0.1
PLA/AII (90/10)	63.0	154.0	0.08	0.1
PLA/AII (80/20)	62.0	153.0	0.13	0.1
PLA/AII (70/30)	62.0	154.0	0.35	0.4
PLA/AII (60/40)	62.0	153.0	0.43	0.5
PLA/AII (50/50)	63.0	153.0	2.10	2.3

Table 3
Tensile testing of unfilled PLA and PLA/AII compositions (filler mean diameter = 9 μm) as determined by stress–strain experiments at r.t. for a crosshead speed of 1 mm/min (standard deviations are given in brackets)

Compositions	Young's modulus (MPa)	Stress at yield (MPa)	Stress at break (MPa)	Nominal strain at break (%)
Processed PLA	436 (43)	65 (2)	61 (1)	9.2 (0.8)
PLA/AII (90/10)	484 (47)	61 (2)	58 (1)	6.1 (0.5)
PLA/AII (80/20)	520 (35)	–	55 (7)	4.6 (0.1)
PLA/AII (70/30)	551 (31)	–	46 (2)	3.9 (0.6)
PLA/AII (60/40)	685 (36)	–	48 (1)	3.3 (0.2)
PLA/AII (50/50)	733 (167)	–	35 (2)	2.5 (0.3)

$$E = E_m\left(1 + 2.5V_f\right) \quad (1)$$

where E and E_m denote the moduli of the composite and incompressible matrix, respectively, and V_f is the volume fraction of filler.

$$\sigma = \sigma_m\left(1 - KV_f^{2/3}\right) \quad (2)$$

where σ and σ_m denote the tensile strengths of the composite and matrix, respectively, and K is a parameter attesting a good adhesion between the filler and matrix for values lower than 1.21.

The linear relationship of the modulus *versus* filler volume fraction plot is consistent with a good interfacial adhesion between PLA and AII (Fig. 5) as well as the K value of 0.84 obtained by fitting the experimental data points with Eq. (2) (Fig. 6). It shows that some favorable interactions are more likely dominant between dried $CaSO_4$ particle surface and ester functions of the PLA backbone.

Such unexpected favorable adhesion properties between AII particles and PLA have been confirmed by impact testing. Indeed, Fig. 7 shows that impact strength is maintained and even slightly improved by incorporating up to 20 wt% AII while the degree of crystallinity of the polyester matrix is

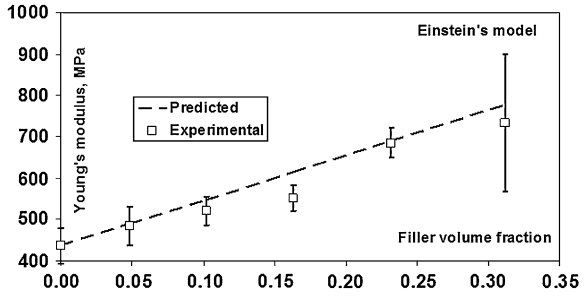

Fig. 5. Plot of Young's modulus *versus* filler volume fraction for PLA/AII compositions (Einstein's prediction: dashed line).

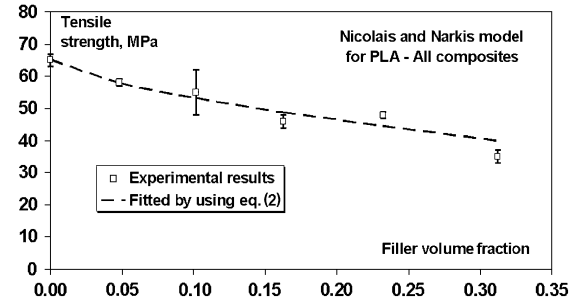

Fig. 6. Plot of tensile strength *versus* filler volume fraction as obtained by fitting the experimental data points via the Nicolais–Narkis equation.

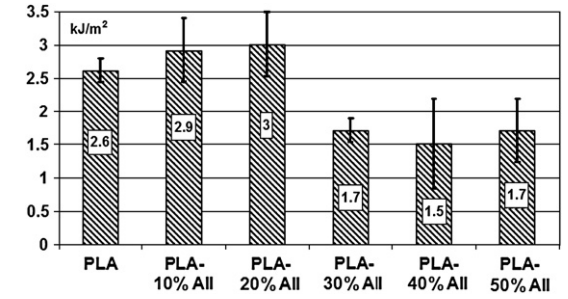

Fig. 7. Notched impact strength (Izod) of neat PLA and PLA/AII compositions.

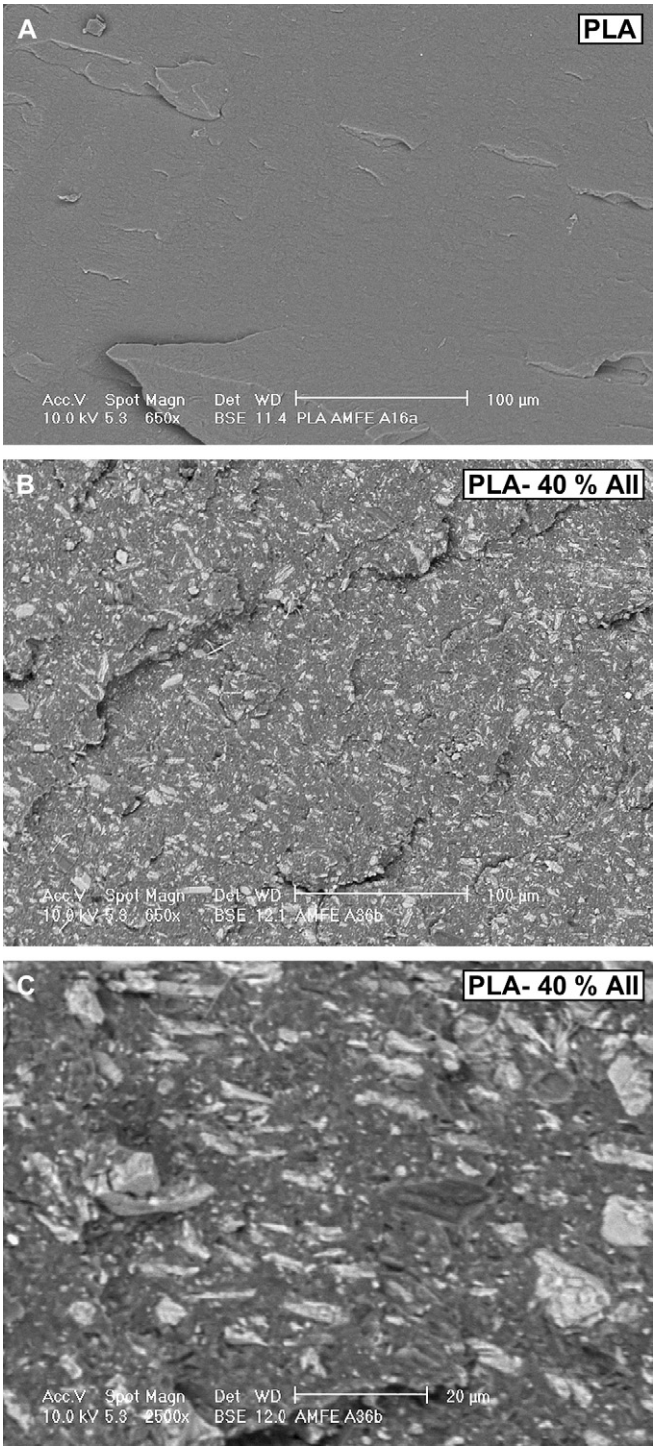

Fig. 8. SEM–BSE pictures of cryofractured surfaces of PLA (A) compared to PLA/AII (60/40) composition at low (B) and high magnifications (C).

kept constant (Table 2). Further increasing the filler content leads to some reduction in the composite toughness and impact strength of 1.7 for PLA/AII (50/50) composition compared to 2.6 kJ/m^2 for the unfilled PLA. With the aim of assessing particles dispersion and particle/polymer interfacial adhesion, SEM images recorded over composite cryofractured surfaces have been performed using back scattered electrons (BSE) to obtain a higher phase contrast. Fig. 8 shows SEM–BSE images of unfilled PLA and PLA/AII (60/40) composition. Well-dispersed β-anhydrite II particles with various geometries and quite broad size distribution are clearly evidenced at the surface of cryofractured composite. A cohesive fracture characterizing moderate but effective adhesion between filler and PLA occurs. It is worth pointing out that such quality of dispersion and interfacial adhesion is obtained without any previous surface treatment of $CaSO_4$ particles. Such behavior is of prime interest in view of decreasing PLA cost and making gypsum by-product profitable for such application as rigid packaging.

4. Conclusion

In response to the demand for enlarging PLA application range while reducing its production cost, this paper demonstrates that commercially available PLA can be effectively melt-blended with previously dried gypsum, actually a by-product directly obtained from the lactic acid fermentation process. Gypsum constitutes a major by-product for which no valuable exploitation had been found yet. Its utilization in plaster is not profitable, competing with less expensive approaches and requires removal of any biological residues, grinding and drying at 100 °C. Therefore, further dehydration of calcium hemihydrate to form β-anhydrite II (AII) might not only be economically viable but can also open the way to PLA/AII compositions with acceptable thermal, mechanical and impact properties. This is due to unexpected favorable interactions existing between $CaSO_4$ and PLA and the ease to obtain highly loaded compositions with well-dispersed filler particles by conventional compounding techniques.

Acknowledgments

Authors thank Galactic s.a., the Wallonia region and European Community for financial support in the frame of INTERREG III: MABIOLAC – "Production of biodegradable composite materials based on lactic acid". They also thank Dr. Y. Paint from Materia Nova for SEM analyses. LPCM is much indebted to both Wallonia region and European Union "FSE and FEDER" for general support in the frame of Objectif-1 Hainaut: Materia Nova, as well as to the Belgian Federal Government Office of Science Policy (SSTC-PAI 5/3) for general support.

References

[1] Vert M. Macromol Symp 2000;153:333–42.
[2] Mochizuki M, Tsuji H. Properties and applications of aliphatic polyester products. In: Doi Y, Steinbüchel A, editors. Biopolymers. Polyesters III. Applications and commercial products. 1st ed. Weinheim: Wiley-VCH Verlag GmbH; 2002. p. 1–23 and 129–77.
[3] Albertsson A-C. Advances in polymer science. In: Degradable aliphatic polyesters, vol. 157. Berlin: Springer Verlag; 2002.
[4] Drumright RE, Gruber PR, Henton DE. Adv Mater 2000;12:1841–6.
[5] Sodergard A, Stolt M. Prog Polym Sci 2002;27(6):1123–63.
[6] Auras R, Harte B, Selke S. Macromol Biosci 2004;4:835–64.
[7] Mecking S. Angew Chem Int Ed 2004;43(9):1078–85.
[8] Degée Ph, Dubois Ph. Recent advances in polylactide chemistry and materials science. In: Kirk-Othmer, editor. Encyclopedia of chemical technology (on line edition). NJ-Hoboken: John Wiley & Sons; 2004.
[9] Narayanan N, Roychoudhury PK, Srivastava A. Electron J Biotechnol 2004;7(2):167–79.
[10] Hong Z, Zhang P, He C, Qiu X, Liu A, Chen L, et al. Biomaterials 2005;26(32):6296–304.
[11] Ignjatovic N, Uskokovic D. Appl Surf Sci 2004;238(1–4):314–9.
[12] Kasuga T, Maeda H, Kato K, Nogami M, Hata K, Ueda M. Biomaterials 2003;24(19):3247–53.
[13] Schiller C, Rasche C, Wehmöller M, Beckmann F, Eufinger H, Epple M, et al. Biomaterials 2004;25(7–8):1239–47.
[14] Niemelä T. Polym Degrad Stab 2005;89(3):492–500.
[15] Shikinami Y, Okuno M. Biomaterials 1999;20(9):859–77.
[16] Bleach NC, Nazhat SN, Tanner KE, Kellomäki M, Törmälä P. Biomaterials 2002;23(7):1579–85.
[17] Prokop A, Jubel A, Helling HJ, Eibach T, Peters C, Baldus SE, et al. Biomaterials 2004;25(2):259–67.
[18] Nicolazo C, Gautier H, Brandao MJ, Daculsi G, Merle C. Biomaterials 2003;24(2):255–62.
[19] Ray SS, Bousmina M. Prog Mater Sci 2005;50(8):962–1079.
[20] van Dijk JAPP, Smit JAM, Kohn FE, Feijen J. J Polym Sci Polym Chem Ed 1983;21(1):197–208.
[21] Fisher EW, Sterzel HJ, Wegner G. Colloid Polym Sci 1973;251:980–90.
[22] Hall ES, Kolstad JJ, Conn RSE, Gruber PR, Ryan CM. U.S. Patent 6,355,772, 2002.
[23] Fatu D. J Therm Anal Calorim 2001;65(1):213–20.
[24] Greco A, Maffezzoli A, Manni O. Polym Degrad Stab 2005;90(2):256–63.
[25] Couturier J. U.S. Patent 6,706,113, 2004.
[26] Cloud ML, Moore KS. U.S. Patent 5,743,728, 1998.
[27] Sievert T, Wolter A, Singh NB. Cement Concr Res 2004;35(4):623–30.
[28] Švab I, Musil V, Leskovac M. Acta Chim Slov 2005;52:264–71.
[29] Bliznakov ED, White CC, Shaw MT. J Appl Polym Sci 2000;77(14):3220–7.